Short Communication

Functional Characterisation of *Dictyostelium* Myosin II with Conserved Tryptophanyl Residue 501 Mutated to Tyrosine

Renu Batra and Dietmar J. Manstein*

Max-Planck-Institut für Medizinische Forschung, Jahnstr. 29, D-69120 Heidelberg, Germany

* Corresponding author

We created a *Dictyostelium discoideum* myosin II mutant in which the highly conserved residue Trp-501 was replaced by a tyrosine residue. The mutant myosin alone, when expressed in a *Dictyostelium* strain lacking the functional myosin II heavy chain gene, supported cytokinesis and multicellular development, processes which require a functional myosin in *Dictyostelium*. Additionally, we expressed the W501Y mutant in the soluble myosin head fragment M761-2R (W501Y-2R) to characterise the kinetic properties of the mutant myosin motor domain. The affinity of the mutant myosin for actin was approximately 6-fold decreased, but other kinetic properties of the protein were changed less than 2-fold by the W501Y mutation. Based on spectroscopic studies and structural considerations, Trp-501, corresponding to Trp-510 in chicken fast skeletal muscle myosin, has been proposed to be the primary ATP-sensitive tryptophanyl residue. Our results confirm these conclusions. While the wild-type construct displayed a 10% fluorescence increase, addition of ATP to W501Y-2R was not followed by an increase in tryptophan fluorescence emission.
Key words: Fluorescence / Molecular motor / Myosin ATPase / Protein engineering.

Spectroscopic methods are widely used to acquire information about conformational changes that occur within the myosin head during ATP hydrolysis and interaction with actin (Trentham *et al.*, 1976). Conformational changes induced by nucleotide binding lead to changes in intrinsic fluorescence and absorption spectra of the environmentally sensitive tryptophanyl residues that can be easily followed. Morita (1967) first demonstrated that the induced difference spectrum observed during ATP hydrolysis was significantly different from that observed in the presence of ADP. Werber *et al.* (1972) further confirmed these results by observing a significant increase in tryptophan fluorescence emission upon binding of various nucleotides to myosin. Bagshaw *et al.* (1974) interpreted the nucleotide

induced enhancement in protein fluorescence to reflect structural changes in the myosin head and proposed a model in the form of the following Scheme where M represents a myosin head fragment, k_{+i} and k_{-i} are the forward and reverse rate constants and K_i (k_{+i}/k_{-i}) is the association equilibrium constant of the i-th step of the reaction.

$$M + T \underset{k_{-1}}{\overset{k_{+1}}{\rightleftharpoons}} M \cdot T \underset{k_{-2}}{\overset{k_{+2}}{\rightleftharpoons}} M^* \cdot T \underset{k_{-3}}{\overset{k_{+3}}{\rightleftharpoons}}$$

$$M^{**} \cdot DP \underset{k_{-4}}{\overset{k_{+4}}{\rightleftharpoons}} M^* \cdot DP \underset{k_{-5}}{\overset{k_{+5}}{\rightleftharpoons}} M^* \cdot D + P \underset{k_{-6}}{\overset{k_{+6}}{\rightleftharpoons}}$$

$$M \cdot D \underset{k_{-7}}{\overset{k_{+7}}{\rightleftharpoons}} M + D$$
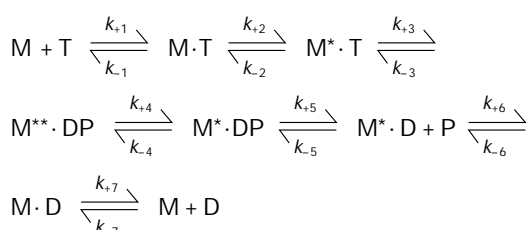
Scheme 1 Model Describing the Mechanism of the Mg^{2+}ATP-Dependent Myosin ATPase.

Step 1 corresponds to the formation of a binary collision complex, followed by an almost irreversible rapid isomerisation to the M*· ATP complex. ATP is then reversibly hydrolysed on the protein (3), and the following rate limiting conformational change (4) limits phosphate release and the faster two-step ADP release (6 and 7). Asterisks refer to the protein conformations with enhanced protein fluorescence. The limiting rate constant for fluorescence enhancement observed at higher [ATP] provides a measure of the rate constant of the hydrolysis step or a conformational change controlling it.

Tryptophanyl fluorescence emission thus has proved empirically useful in the kinetic analysis of myosin, but it was only within the last decade that attempts were made to identify the residues responsible (Papp and Highsmith, 1993; Burghardt and Ajtai, 1996). Based on fluorescence resonance energy transfer studies used to detect small movements that occur in protein upon ligand binding, Johnson *et al.* suggested Trp-510 and Trp-594 in the 50 kDa fragment of the myosin head to correspond to the ATP-perturbable tryptophans (Johnson *et al.*, 1991). In another set of similar studies, Hiratsuka (1992) proposed Trp-510 to be the most likely ATP-sensitive residue. This conclusion was based on examining the fluorescence energy transfer between the ATP-sensitive tryptophanyl residue(s) and a [2-(4′-maleimidylanilino)-napthalene-6-sulfonic acid] fluorophore attached to the SH2 reactive thiol residue of rabbit skeletal myosin. Burghardt and coworkers extended this approach using xanthene probes that bind specifically to the SH1 reactive thiol residue of skeletal myosin and showed that fluorescence emission

from Trp-510 was completely quenched as a result of the SH1-modification (Park *et al.*, 1996). The authors further suggested that a one-to-one correlation exists between Trp-510 conformation and transient states of myosin during contraction. That Trp-510 is responsible for the changes in protein fluorescence upon binding of ATP is also implied by structural studies. The loop containing Trp-510 displays high sequence conservation and forms the major coupling element between the nucleotide binding site, the converter-lever arm system and the actin binding site (Figure 1). Depending on the state of the nucleotide bound in the active site, Trp-510 is either buried or exposed to the solvent (Smith and Rayment, 1996; Dominguez *et al.*, 1998).

Here we describe the generation and characterisation of a *Dictyostelium* myosin II mutant in which Trp-501 was replaced by a tyrosine residue. Trp-501 of *Dictyostelium* myosin II corresponds to Trp-510 of rabbit skeletal muscle

Fig. 1   Ribbon Representation of the Structure of the Globular Head Domain of *Dictyostelium* Myosin II Complexed with ADP·BeF$_3$ (Schlichting, I., Kull, F.J., Manstein, D.J., and Holmes, K.C. unpublished results).

The model is oriented to show all tryptophanyl residues. Residues W36, W432 and W584 are shown in yellow and residue W501 in orange. Residues 1–210 forming the 25 kDa domain are shown in green, residues 211–460 forming the upper 50 kDa domain in red, residues 461–630 forming the lower 50 kDa domain in white and residues 631–754 forming the 20 kDa domain in blue. The SH1- and SH2-helices are shown in light blue. The nucleotide is shown in spacefilling mode and coloured in magenta. The Figure was produced using the program RasMol 2.6 (R.A. Sayle, Glaxo Wellcome Research and Development).
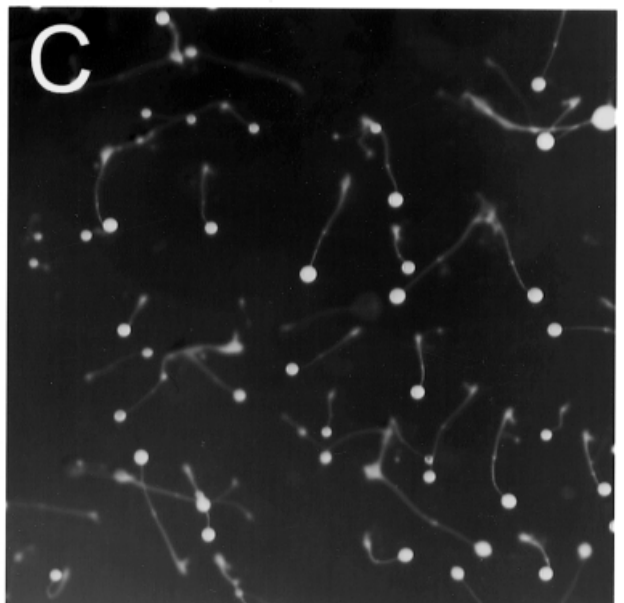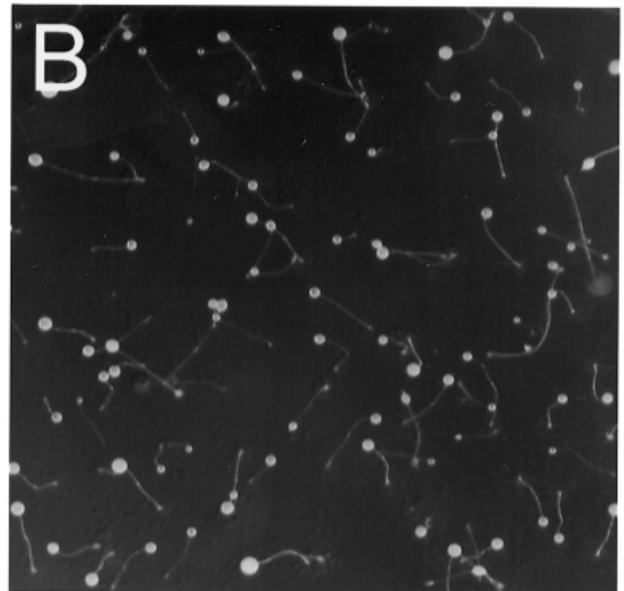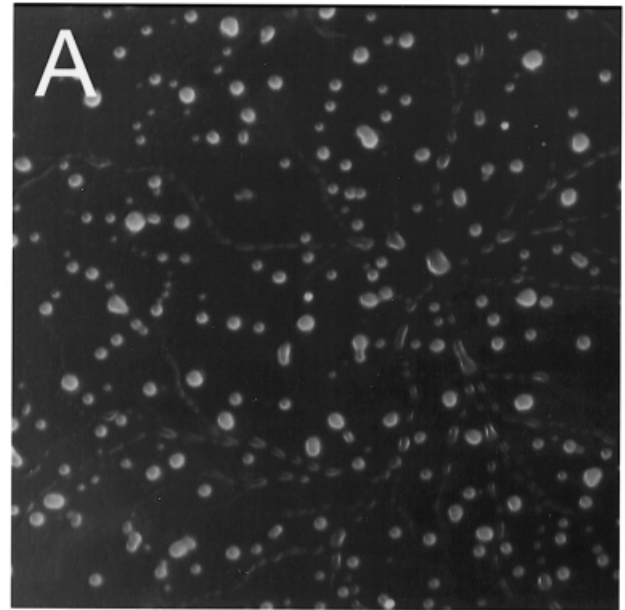
Table 1   Steady-State ATPase Activities of Mutant and Wild-Type Myosin Head Fragments.

Construct	Basal Mg^{2+}-ATPase (s^{-1})	High-salt Ca^{2+}-ATPase (s^{-1})	Actin-activated Mg^{2+}-ATPase		
			K_{app} (μM)	k_{cat} (s^{-1})	k_{cat}/K_{app} ($M^{-1}\,s^{-1}$)
M761-2R	0.12	1.0	110	2.7	0.25×10^5
W501Y-2R	0.13	0.4	121	1.2	0.98×10^4

All measurements were performed at 30 °C . Experimental conditions were as described by White (1982).

myosin. Both a mutant version of full-length myosin and of the soluble myosin head fragment M761-2R (M761-2R is a recombinant protein corresponding to the myosin catalytic domain fused to two α-actinin repeats; Anson *et al.*, 1996) were produced. The mutant version of M761-2R (W501Y-2R) was produced with a C-terminal His-tag to facilitate purification by Ni^{2+}-chelate affinity chromatography (Janknecht *et al.* 1991; Manstein and Hunt, 1995). Typically, 2 mg of pure protein was obtained from 1 g of cells producing either construct.

In the *Dictyostelium* system the functionality of a mutant myosin can be easily assessed *in vivo*. Cytokinesis and fruiting body formation are processes that require a functional myosin in *Dictyostelium* (Knecht and Loomis, 1987; De Lozanne and Spudich, 1987). Transformants expressing W501Y-myosin were able to divide in suspension culture with a doubling time comparable to that of wild-type cells and recovered the ability to form fruiting bodies (Figure 2).

ATP turnover by M761-2R and W501Y-2R was measured under three different conditions, namely basal ATPase, actin-activated ATPase and Ca^{2+}-high salt ATPase. The first two were measured under low salt con-

ditions and in the presence of Mg^{2+} (Table 1). Basal ATPase activities of M761-2R and W501Y-2R motor domains were similar with turnover rates of 0.12 s^{-1}.

Actin activation of the ATPase activity was examined over a wide range of actin concentrations (0–80 μM). At concentrations of actin much lower than K_{app}, the dependence of the apparent ATPase rate on actin concentration could be fitted to a straight line and the apparent second order rate constant (k_{cat}/K_{app}) of the reaction was determined from the slope of this line. Values for K_{app} and k_{cat} were obtained from fitting the data to the Michaelis-Menten equation. The values obtained for k_{cat} and k_{cat}/K_{app} were 2.5-fold lower than those obtained with M761-2R (Table 1). Similarly, the Ca^{2+}-ATPase activity measured for W501Y-2R was 0.4 s^{-1}, 2.5-fold lower than the rate of 1.0 s^{-1} measured for M761-2R.

In the case of rabbit S1, a protein fluorescence change that follows the addition of ATP is thought to monitor two distinct steps: a fluorescence increase on ATP binding followed by a further increase concomitant with ATP hydrolysis (Bagshaw and Trentham, 1974). Unlike S1, *Dictyostelium* myosin II motor domain constructs do not display a fluorescence change upon ADP binding (Ritchie *et al.*, 1993). Based on this observation and the absence of two tryptophans residues in the nucleotide binding site of *Dictyostelium* myosin II, it was suggested that for *Dictyostelium* myosin II the signal change results only from the

---

Fig. 2   Formation of Fruiting Bodies.
(A) *Dictyostelium* myosin null cells; (B) myosin null cells transformed with a expression vector for the production of W501Y-myosin; (C) *Dictyostelium* wild-type cells. The morphogenetic changes of the myosin null cells are arrested early in development at the 'mound stage', whereas wild-type cells and cells producing W501Y-myosin form normal fruiting bodies.

The expression vectors used for the production of mutant myosin constructs are based on pDXA-3H (Manstein *et al.*, 1995). The point mutation was introduced in M761-2R, a fusion construct comprised of the first 761 residues of the *Dictyostelium* myosin II heavy chain linked to codon 264 and extending to codon 505 of the *Dictyostelium* α-actinin gene. All constructs were tagged at their carboxy-termini with the peptide Asp-Ala-Leu-(His)$_8$. The plasmid encoding W501Y-2R was created by site-directed mutagenesis using the Quick-change kit (Stratagene, Heidelberg, Germany). The oligonucleotides used to PCR-amplify the mutant myosin was: W501Y (5'CTTAAAGAGAAAATCAATT**AT**ACTTTC-ATCGATTTTGGTCTTG) with the mutated residues underlined. The full-length mutant construct was created by replacing the *Sal*I/*Bst*X1 fragment of pDH4 with the fragment containing the point mutation. The plasmid pDH4 encodes the complete myosin II heavy chain fused to an N-terminal His$_7$-tag. Molecular genetic manipulations of *Dictyostelium* were performed as described by Egelhoff *et al.* (1991) and all myosin constructs were confirmed by DNA sequencing.
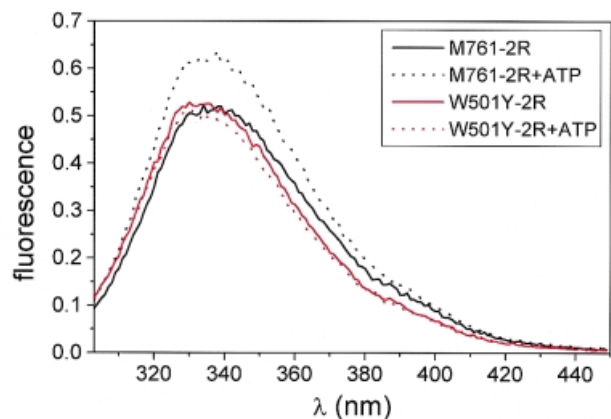
Fig. 3   Fluorescence Emission Spectra of Myosin Motor Domain Constructs M761-2R and W501Y-2R in the Absence and Presence of ATP (2 mM).
Fluorescence emission spectra were recorded at 20 °C in an SLM 8000 fluorescence spectrophotometer. The slit widths of excitation and emission monochromators were 4 nm. Tryptophan fluorescence was excited at 290 nm.

hydrolysis step (Ritchie *et al.*, 1993). The fluorescence emission spectra of W501-2R and M761-2R are shown in Figure 3. Tryptophanyl residues, when excited at 290 nm, fluoresce in the region 300–400 nm with a maximum at 334 nm. Upon addition of 2 mM ATP to 2 μM protein, the fluorescence of M761-2R increased by 25% while that of W501Y-2R decreased by 3% (Figure 3A). The amplitude of the fluorescence signal showed little change between 50 μM and 2 mM ATP. The rate of ATP binding to myosin was measured using the stopped-flow technique. Following the addition of an excess of ATP, a 10% increase in tryptophanyl fluorescence was observed for M761-2R while no fluorescence change was observed with W501Y-2R (Figure 4). We have previously reported similar rates of ATP and mant [2-(3-)-O-(*N*-methylanthraniloyl)]-ATP binding to *Dictyostelium* myosin head fragments including M761-2R (Kurzawa *et al.*, 1997). Therefore, the rate of mantATP binding to W501Y-2R was monitored from the increase in fluorescence following addition of substoichiometric concentrations of mantATP. A 2.2-fold enhancement of fluorescence was observed with both M761-2R and W501Y-2R upon mantATP binding. The observed process could be fitted to a single exponential $[F = F_0 (1 - e^{-k_{obs}t})]$ (Figure 5A). The observed rate constant (k_{obs}) was linearly dependent on the concentration of mant-
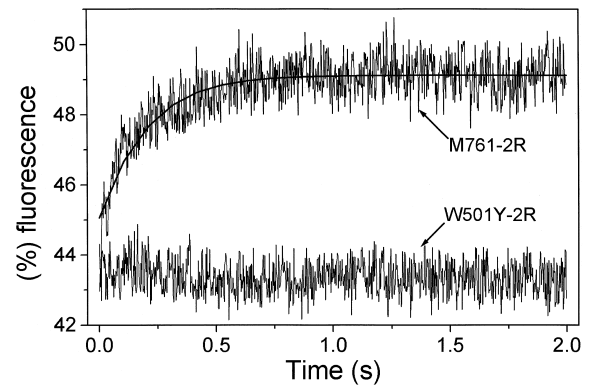
Fig. 4 Stopped-Flow Records Following the Addition of ATP to the Myosin Motor Domain Constructs.

Stopped-flow experiments were performed for transient kinetic measurements at 20 °C with a Hi-Tech SF61 stopped-flow spectrophotometer equipped with a 100 W Xe/Hg lamp and a monochromator. Fluorescence was excited at 295 nm and emission was observed through a WG 320 filter. Data were stored and analysed using software provided by Hi-Tech Scientific (Salisbury, U.K.). Transients shown are the average of three to five consecutive shots of the stopped-flow device. Binding of 10 μM Mg²⁺-ATP to 0.5 μM M761-2R and W501Y-2R was recorded. All concentrations refer to the concentration of the reactants after mixing in the stopped-flow observation cell. The experimental buffer was 20 mM MOPS, 5 mM MgCl₂ and 100 mM KCl, pH 7.0.
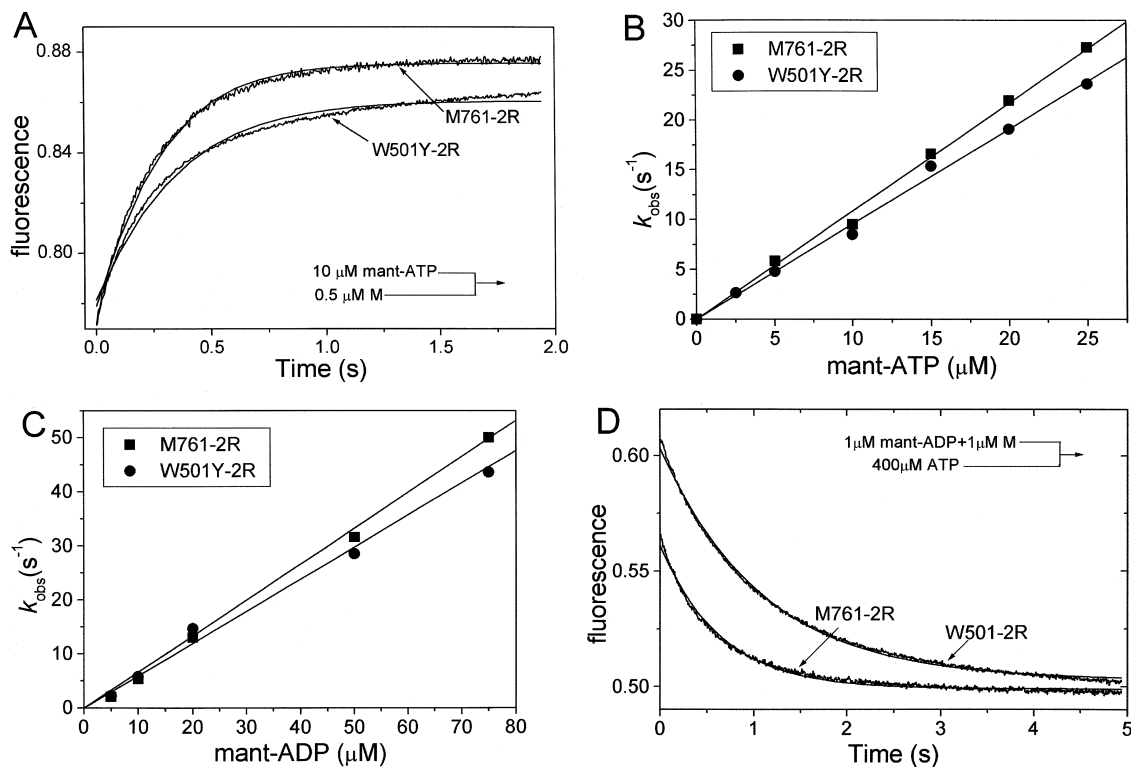
Fig. 5 Interaction of the Myosin Motor Domain Constructs with Mant-nucleotides.
(A) Fluorescence change on 10 μM mant ATP binding to 0.5 μM M761-2R and W501Y-2R in the stopped-flow fluorometer. (B) Dependence of the observed rate constant of the fluorescence change on [mantATP]. (C) Dependence of the observed rate constant of the fluorescence change on [mantADP]. The data for mantADP- and mantATP-binding were fitted to a straight line. The second order rate constants for mantATP binding ($K_1 K_{+2}$) and mantADP binding (k_{+D}) were derived from the slopes of these best-fit lines. (D) Rate of ADP displacement from myosin head fragments. Stopped-flow record of fluorescence decrease during binding of 400 μM ATP to 1.0 μM MHF, premixed with 1 μM mantADP.
Fluorescence was excited at 365 nm with emission detection through a KV 389 filter. The rate constants are summarised in Table 2.

ATP in the range 5–25 μM. The second order rate constant ($K_1 k_{+2}$) is defined by the slope of the best-fit line shown in Figure 5B. The $K_1 k_{+2}$ values obtained were similar for M761-2R and W501Y-2R (Table 2).

Binding of mantADP to the myosin head fragments was monitored by observing the exponential increase in fluorescence. The observed rate constant was linearly dependent on the concentration of mantADP over the range 5–50 μM. The second order rate constant was measured from the slope of the plot obtained in Figure 5C and the values obtained for M761-2R and W501Y-2R were comparable (Table 2). The rate of mantADP displacement was measured by monitoring the decrease in fluorescence upon ATP-induced mantADP release from the M·mantADP complex. Rates of mantADP release (k_{-D}) measured for M761-2R and W501Y-2R were 2.6 s^{-1} and 2.0 s^{-1} (Figure 5D, Table 2).

Since the excitation spectrum of mantATP closely overlaps the emission spectrum of tryptophan residues, mantATP, when bound to myosin fragments, can also be excited at 295 nm (Millar and Geeves, 1988; Ritchie et al., 1993). In the case of M761-2R and W501-2R, identical fluorescence time courses and signal amplitudes were observed when mantATP fluorescence was excited directly or indirectly. There are only three tryptophan residues in the *Dictyostelium* myosin motor domain that can be responsible for the transfer of energy to mantATP, as the equivalent residues to W113 and W131 in chicken skeletal myosin are D112 and R130 in the *Dictyostelium* myosin II heavy chain sequence. The remaining tryptophan residues W36, W432, and W584 (see Figure 1) are positioned at similar distances of 25 to 30 Å from the adenosine moiety in the various *Dictyostelium* myosin motor domain structures complexed with different nucleotides (Fisher et al. 1995; Smith and Rayment, 1995; Gulick et al. 1997).

Table 2   Results of the Transient Kinetic Analysis.

	Rate constant	M761-2R	W501Y-2R
Nucleotide* binding to MHF	$K_1 k_{+2}$ (M^{-1} s^{-1})	1.1×10^6	0.97×10^6
	k_{+D} (M^{-1} s^{-1})	6.7×10^5	5.9×10^5
	k_{-D} (s^{-1})	2.6	1.96
	K_D (μM) (k_{-D}/k_{+D})	3.9	3.3
Nucleotide* binding to acto·MHF	$K_1 k_{+2}$ (M^{-1} s^{-1})	1.55×10^5	0.85×10^5
	K_1 (M^{-1})	250	180
	k_{+2} (s^{-1})	504	340
	K_{AD} (μM)	215	186
Actin binding to MHF	k_{+A} (M^{-1} s^{-1})	1.3×10^6	0.68×10^6
	k_{-A} (s^{-1})	5.6×10^{-3}	17.7×10^{-3}
	$K_A = k_{-A}/k_{+A}$ (nM)	4.3	26

The experiments were analysed in terms of the models shown in Schemes 1 and 2. A notation is used that distinguishes between the constants in the presence and absence of actin by using bold letters (k_{+1}, K_1) versus italics (k_{+1}, K_1); subscript 'A' and 'D' refer to actin (K_A) and ADP (K_D), respectively.
Experimental conditions: 20 mM MOPS, 5 mM MgCl$_2$, 100 mM KCl, pH 7.0, 20 °C.
* Mantanalogue.

The rate of actin binding was measured by following the exponential decrease in pyrene fluorescence observed upon binding of excess pyr-actin (actin labelled with pyrene-iodoacetamide on Cys-374) to the respective myosin motor domain construct (Kurzawa and Geeves, 1996). The observed rate constants were plotted against the pyr-actin concentration and for both M761-2R and W501Y-2R, k_{obs} was linearly dependent on the actin concentration over the range studied (0.5–3.0 μM). The second order rate constant for pyr-actin binding (k_{+A}) obtained was 2-fold slower for W501Y-2R than for M761-2R (Table 2).

The rate of actin dissociation (k_{-A}) from the myosin motor domains was determined by chasing pyr-actin bound to the respective myosin motor domain construct with an excess of unlabelled actin (Figure 6A and B). The observed process could be fitted to a single exponential where k_{obs}
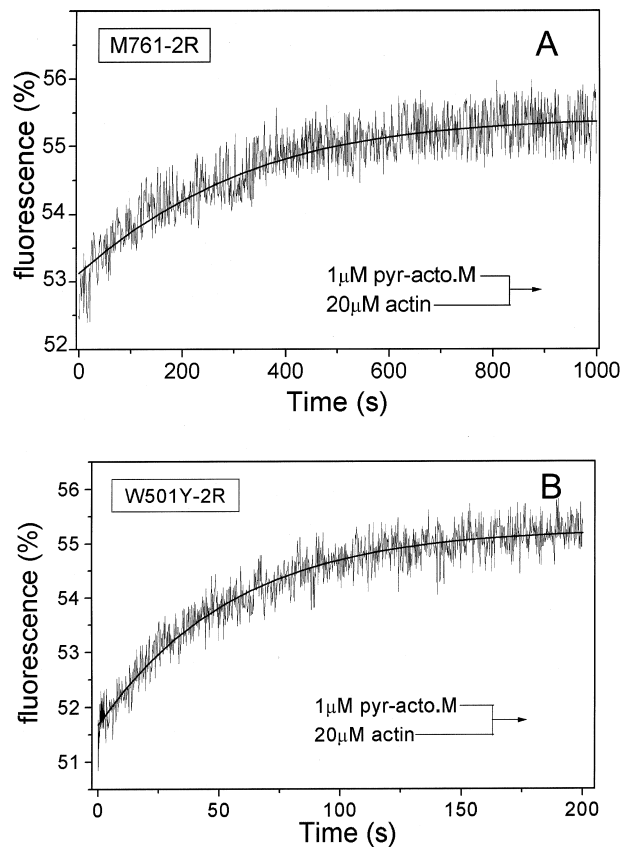
Fig. 6 Determination of the Rate of Actin Displacement from acto·M761-2R and pyr-acto·W501Y-2R.
(A) Stopped-flow records showing the rate of actin dissociation from the complex with M761-2R. (B) Stopped flow records showing the rate of actin dissociation from the complex with W501Y-2R.
The dissociation rate constant (k_{-A}) was determined from the rate of fluorescence enhancement when excess unlabelled actin was added to a sample of 0.5 μM pyr-actin equilibrated with an equimolar amount of myosin motor domain peptide. The solid lines are the best fit to single exponential functions and define the values for k_{-A} shown in Table 2. Rabbit actin was purified by the method of Lehrer and Kewar (1972) and labelled with pyrene actin as previously described (Criddle et al., 1985).

corresponds directly to k_{-A}. The rate of actin dissociation from W501Y-2R was approximately 3-fold faster than that obtained for M761-2R (Table 2). The dissociation equilibrium constant for actin binding (K_A) was calculated from the ratio of k_{-A}/k_{+A}. Values of 4.3 nM for M761-2R and 26 nM for W501Y-2R were obtained.

Nucleotide binding in the presence of actin was analysed in terms of models developed by Millar and Geeves (1983) and Siemankowski and White (1984):

$$A \cdot M + ATP \xrightleftharpoons{K_1} A \cdot M \cdot ATP \xrightarrow{k_{+2}} A + M \cdot ATP$$

$$A \cdot M \cdot ADP \xrightleftharpoons{K_{AD}} A \cdot M + ADP$$
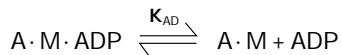
Scheme 2   Model Describing the Mechanism of the Acto· M ATPase.

A and M represent actin and myosin head fragment, respectively. The first step after mixing acto· M and ATP is the rapid equilibration between A· M and ATP defined by the equilibrium constant K_1, this is followed by an isomerization of the ternary complex which limits the maximum rate of actin dissociation from the complex. Thus the observed rate constant for the ATP induced dissociation of actin from the complex is defined by $k_{obs} = [ATP]K_1k_{+2}/1 + K_1[ATP]$.

The binding of ATP to pyr-acto· M complexes was monitored by observing the exponential increase in pyrene fluorescence following addition of excess ATP. The observed rate constants were linearly dependent upon ATP concentrations in the range of 5–25 μM as shown in Figure 7A. The second order binding constants K_1k_{+2}, defined by the gradient in Figure 7A, differ by less than 2-fold for M761-2R and W501Y-2R (Table 2). At high ATP concentrations (>2 mM) the observed rate constants saturate and the [ATP] dependence of k_{obs} could be described by a hyperbola as predicted by Scheme 2, where $k_{max} = k_{+2}$ and $K_{0.5} = 1/K_1$ (Figure 7B). The data obtained with W501Y-2R are again very similar to those obtained for M761-2R, with both K_1 and k_{+2} varying by less than a factor of 2.

The affinity of ADP for pyr-acto· M was determined from the competitive inhibition of ATP-induced dissociation of pyr-acto· M. Again the exponential increase in pyrene fluorescence during the dissociation of the pyr-acto· M complex was monitored. Assuming a rapid equilibrium between A· M and the ADP bound state, for a fixed ATP concentration the k_{obs} is given by the equation $k_{obs} = k_0/(1 + [ADP]/K_{AD})$, where k_0 is the observed rate constant in the absence of ADP and the dissociation constant K_{AD} represents the affinity of ADP for the actomyosin complex (Siemankowski and White, 1984). Dissociation constants of approximately 200 μM were obtained for both constructs (Figure 7C, Table 2).

Here we have used a multifaceted approach that includes site-directed mutagenesis, transient kinetics, and cell biological techniques to investigate the role of the highly conserved tryptophan residue in the relay loop of myosin. Our results show that the mutant protein is little
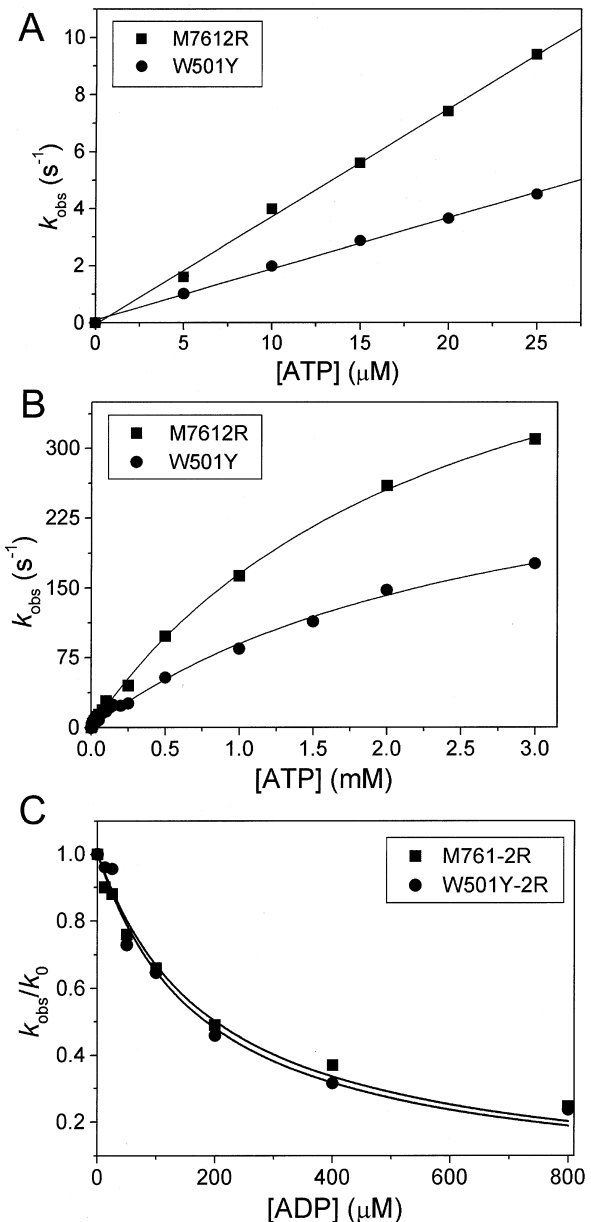
Fig. 7   Interaction of Nucleotides with pyr-acto· M761-2R and pyr-acto· W501Y-2R.

(A) ATP-induced dissociation of acto· M complexes. Plot of k_{obs} *versus* ATP concentration. The observed rate constants are linearly dependent on [ATP] in the range 5–25 μM. (B) At higher ATP concentrations the data were fitted to a hyperbola. (C) Competitive binding of ATP and ADP to pyr-acto· M. Plot of k_{obs}/k_0 *versus* ADP concentration. The dissociation constants of the ADP complexes were determined by fitting the plot to the equation $k_{obs}/k_0 = 1/(1 + [ADP]/K_{AD})$; k_0 is the observed rate constant in the absence of ADP.

altered in its kinetic and functional properties. The only major difference is a 6-fold decrease in actin affinity in the absence of nucleotide. Our observation that replacement of residue Trp-501 with a tyrosine residue results in complete loss of intrinsic fluorescence enhancement upon ATP binding confirms previous studies (Hiratsuka, 1992; Park *et al.*, 1996) that assigned the relay loop tryptophan to be the ATP-sensitive tryptophan.

Acknowledgements

References

Anson, M., Geeves, M.A., Kurzawa, S.E., and Manstein, D.J. (1996). Myosin motors with artificial lever arms. EMBO J. *15*, 6069–6074.

Bagshaw, C.R., Eccleston, J.F., Eckstein, F., Goody, R.S., Gutfreund, H., and Trentham, D.R. (1974). The magnesium ion-dependent adenosine triphosphatase of myosin. Two-step processes of adenosine triphosphate association and adenosine diphosphate dissociation. Biochem. J. *141*, 351–364.

Burghardt, T.P., and Ajtai, K. (1996). The conformation of xanthene dyes in the myosin sulfhydryl one binding site. Part I. Methods and model systems. Biophys. Chem. *60*, 119–133.

Criddle, A.H., Geeves, M.A., and Jeffries, T. (1985). The use of actin labelled with N-(1-pyrenyl)iodoacetamide to study the interaction of actin with myosin subfragments and troponin/tropomyosin. Biochem. J. *232*, 343–349.

De Lozanne, A., and Spudich, J.A. (1987). Disruption of the *Dictyostelium* myosin heavy chain gene by homologous recombination. Science *236*, 1086–1091.

Dominguez, R., Freyzon, Y., Trybus, K. M., and Cohen, C. (1998). Crystal structure of a vertebrate smooth muscle myosin motor domain and its complex with the essential light chain: Visualization of the pre-power stroke state. Cell *94*, 559–571.

Egelhoff, T.T., Titus, M.A., Manstein, D.J., Ruppel, K.M., and Spudich, J.A. (1991). Molecular genetic tools for study of the cytoskeleton in *Dictyostelium*. Methods Enzymol. *196*, 319–334.

Fisher, A.J., Smith, C.A., Thoden, J.B., Smith, R., Sutoh, K., Holden, H.M., and Rayment, I. (1995). X-ray structure of the myosin motor domain of *Dictyostelium discoideum* complex with MgADP·BeF$_x$ and MgADP·AlF$_4^-$. Biochemistry *34*, 8960–8972.

Gulick, A.M., Bauer, C.B., Thoden, J.B., and Rayment, I. (1997). X-ray structures of the Mg-ADP, Mg-ATPγS, and Mg-AMPPNP complexes of the *Dictyostelium discoideum* myosin motor domain. Biochemistry *36*, 11619–11628.

Hiratsuka, T. (1992). Spatial proximity of ATP-sensitive tryptophanyl residue(s) and Cys-697 in myosin ATPase. J. Biol. Chem. *267*, 14949–14954.

Janknecht, R., de Martynoff, G., Lou, J., Hipskind, R.A., Nordheim, A., and Stunnenberg, H.G. (1991). Rapid and efficient purification of native histidine-tagged protein expressed by recombinant vaccinia virus. Proc. Natl. Acad. Sci. USA *88*, 8972–8976.

Johnson, W.C., Jr., Bivin, D.B., Ue., K., and Morales, M. F. (1991). A search for protein structural changes accompanying the contractile interaction. Proc. Natl. Acad. Sci. USA *88*, 9748–9750.

Knecht, D.A., and Loomis, W. F. (1987). Antisense RNA inactivation of myosin heavy chain gene expression in *Dictyostelium discoideum*. Science *236*, 1081–1086.

Kurzawa, S.E., and Geeves, M.A. (1996). A novel stopped-flow method for measuring the affinity of actin for myosin head fragments using microgram quantities of protein. J. Muscle Res. Cell Motil. *17*, 9–676.

Kurzawa, S.E., Manstein, D.J., and Geeves, M.A. (1997). *Dictyostelium discoideum* myosin II: characterization of functional myosin motor fragments. Biochemistry *36*, 317–323.

Lehrer, S.S., and Kewar, G. (1972). Intrinsic fluorescence of actin. Biochemistry *11*, 1211–1217.

Manstein, D.J., and Hunt, D.M. (1995). Overexpression of myosin motor domains in *Dictyostelium*: screening of transformants and purification of the affinity tagged protein. J. Muscle Res. Cell Motil. *16*, 325–332.

Manstein, D.J., Schuster, H.-P., Morandini, P., and Hunt, D.M. (1995). Cloning vectors for the production of proteins in *Dictyostelium discoideum*. Gene *162*, 129–134.

Millar, N. C., and Geeves, M. A. (1983). The limiting rate of the ATP-mediated dissociation of actin from rabbit skeletal muscle myosin subfragment 1. FEBS Lett. *160*, 141–148.

Morita, F. (1967). Interaction of heavy meromyosin with substrate. I. Difference in ultraviolet absorption spectrum between heavy meromyosin and its Michaelis-Menten complex. J. Biol. Chem. *242*, 4501–4506.

Papp, S.J., and Highsmith, S. (1993). The ATP-induced myosin subfragment-1 fluorescence intensity increase is due to one tryptophan. Biochim. Biophys. Acta *1202*, 169–172.

Park, S., Ajtai, K., and Burghardt, T. P. (1996). Optical activity of a nucleotide-sensitive tryptophan in myosin subfragment 1 during ATPase hydrolysis. Biphysical Chem. *63*, 67–80.

Ritchie, M.D., Woodward, S.K.A., Manstein, D.J., and Geeves, M.A. (1993). Characterization of the interaction of a *Dictyostelium* myosin head fragment with actin and nucleotide. Biophys. J. *64*, 359–359.

Siemankowski, R.F., and White, H.D. (1984). Kinetics of the interaction between actin, ADP, and cardiac myosin-S1. J. Biol. Chem. *259*, 5045–5053.

Smith, C.A., and Rayment, I. (1995). X-ray structure of the magnesium(II)-pyrophosphate complex of the truncated head of *Dictyostelium discoideum* myosin at 2.7 Å resolution. Biochemistry *34*, 8973–8981.

Smith, C.A., and Rayment, I. (1996). X-ray structure of the magnesium(II).ADP. vanadate complex of the *Dictyostelium discoideum* myosin motor domain to 1.9 Å resolution. Biochemistry *35*, 5404–5417.

Trentham, D.R., Eccleston, J.F., and Bagshaw, C.R. (1976). Kinetic analysis of ATPase mechanisms. Q. Rev. Biophys. *9*, 217–281.

Werber, M. M., Szent-Györgyi, A.G., and Fasman, G.D. (1972). Fluorescence studies on heavy meromyosin-substrate interaction. Biochemistry *11*, 2872–2883.

White, H.D. (1982). Special instrumentation and techniques for kinetic studies of contractile systems. Methods Enzymol. *85*, 698–708.